

Brilliant Blue G Protects against Rotenone-Induced Neuronal Damage in the Rat Brain

Omar M.E. Abdel-Salam¹, Eman R. Youness², Nadia A. Mohammed², Noha N. Yassen³, Nermeen Shaffie³, and Amany A. Sleem⁴

¹Department of Toxicology and Narcotics, ²Department of Medical Biochemistry, ³Department of Pathology, ⁴Department of Pharmacology, National Research Centre, Cairo, Egypt

Correspondence: omasalam@hotmail.com (O.M.A-S.)

Abdel-Salam O.M. et al. Reactive Oxygen Species 4(11):336–350, 2017; ©2017 Cell Med Press
<http://dx.doi.org/10.20455/ros.2017.855>
 (Received: June 30, 2017; Accepted: July 5, 2017)

ABSTRACT | We aimed to investigate the effect of brilliant blue G on the development of oxidative stress and neuronal damage in rat brain after the systemic administration of rotenone. Rats were subcutaneously (s.c.) injected with rotenone (1.5 mg/kg) alone or in combination with brilliant blue G (5 or 10 mg/kg) every other day for two weeks. The control group received the vehicle (dimethyl sulfoxide). Biochemical markers of oxidative stress: malondialdehyde, reduced glutathione, nitric oxide, paraoxonase-1 (PON-1), and nuclear factor kappaB (NF-κB) were determined in the brain. Rotenone caused markedly increased lipid peroxidation, as assessed by malondialdehyde. In addition, brain nitric oxide concentrations were markedly increased while reduced glutathione concentrations and PON-1 activity decreased compared with the vehicle-treated group. Rats treated with only rotenone also showed a significant increase in brain NF-κB levels. In vehicle-treated rats, the administration of brilliant blue G at 10 mg/kg had no significant effect on brain malondialdehyde, reduced glutathione, nitric oxide concentrations, NF-κB, or PON-1 activity. In rotenone-treated rats, brilliant blue G given at 5 or 10 mg/kg had no significant effect on brain malondialdehyde or reduced glutathione levels. Treatment with brilliant blue G at 10 mg/kg, however, reduced the brain concentration of nitric oxide by 39.6% and increased PON-1 activity by 76.5%. NF-κB was reduced by 19.1% and 19.5% by 5 and 10 mg/kg brilliant blue G, respectively. Rotenone caused neuronal atrophy in the cerebral cortex and hippocampus, and decreased the number of pigmented neurons in the substantia nigra. There were significantly increased cleaved caspase-3 immunoreactivity and decreased number of glial fibrillary acidic protein (GFAP)-positive astrocytes in cerebral cortex. In rats treated with rotenone, brilliant blue G attenuated neurodegeneration, decreased caspase-3 immunoreactivity, and rescued GFAP-positive astrocytes. These data show that brilliant blue G exhibits antiapoptotic and neuroprotective effect against the rotenone neurotoxicity. This action of brilliant blue G is likely to involve an inhibitory effect on brain nitric oxide and NF-κB.

KEYWORDS | Apoptosis; Astrocytes; Brilliant blue G; Neuroprotection; Oxidative stress; Rotenone

ABBREVIATIONS | GFAP, glial fibrillary acidic protein; GSH, reduced glutathione; iNOS, inducible nitric oxide synthase; NF-κB, nuclear factor kappaB; nNOS, neuronal nitric oxide synthase; PD, Parkinson's disease; PON-1, paraoxonase-1; sc, subcutaneous injection; SNPc, substantia nigra pars compacta

CONTENTS

1. Introduction
2. Materials and Methods
2.1. Animals
2.2. Drugs and Chemicals
2.3. Study Design
2.4. Biochemical Analyses
2.4.1. Determination of Lipid Peroxidation
2.4.2. Determination of Reduced Glutathione
2.4.3. Determination of Nitric Oxide
2.4.4. Determination of Paraoxonase-1 Activity
2.4.5. Quantification of Nuclear Factor kappaB
2.5. Histopathological Assessment Studies
2.6. Immunohistochemistry for Caspase-3 and Glial Fibrillary Acidic Protein
2.7. Immunomorphometric Analysis
2.8. Detection of Caspase-3 and GFAP Percentage Area
2.9. Statistical Analysis
3. Results
3.1. Oxidative Stress
3.2. PON-1 Activity
3.3. Nuclear Factor kappaB
3.4. Histopathological Results
3.5. Immunohistochemistry Results
3.6. Immunomorphometric Results
4. Discussion

1. INTRODUCTION

Parkinson's disease (PD) is a progressive neurodegenerative disorder for which there is no cure [1, 2]. The disease is essentially sporadic with only ~5% being of genetic origin [3, 4]. This age-related disorder occurs in ~1% of the population over the age of 65 years [5]. In PD, the pigmented dopaminergic neurons of the substantia nigra pars compacta (SNPc) of the midbrain undergo selective and continued death. The result is profound dopamine deficiency in the SNPc and striatum with emergence of the motor manifestations of the disease, i.e., bradykinesia, muscular rigidity, and hand tremor [6, 7]. The death of the dopaminergic neurons is largely thought to be driven by oxidative/nitrosative stress and neuroinflammation [8, 9]. Reactive oxygen metabolites are normally produced as a result of cellular respiration. The most important source is the electron transport chain of the mitochondria, where the mitochondrial complexes I and II leak electrons to molecular oxygen forming superoxide anion radical

(O₂^{•-}). In turn, superoxide can result in the formation of several intermediates such as hydrogen peroxide (H₂O₂), and hydroxyl radical (OH[•]) or react with nitric oxide to generate the highly reactive peroxynitrite anion (ONOO⁻) [10, 11]. The brain is particularly susceptible to free radical-mediated oxidative damage [10, 12]. Several factors account for this high susceptibility including the brain's high rate of oxygen consumption, the rich content of polyunsaturated fatty acids, and the presence of the redox-active transition metals (iron and copper) [10, 12]. Moreover, the autoxidation of dopamine results in the formation of redox active dopamine quinones or semiquinones radicals which can then lead to the formation of the superoxide radical, hydrogen peroxide, and the hydroxyl radical [13, 14]. The brain is also relatively deficient in antioxidant mechanisms when compared to other tissues [12]. In PD brain, there is misassembly and reduced catalytic activity of the mitochondrial complex I [15, 16]. The latter is the main source for superoxide formation in the brain and an increase in the generation of reactive oxygen

metabolites by the mitochondrial electron transport chain follows inhibition of complex I [17, 18]. The presence of neuroinflammation also contributes to neuronal damage in PD where activation of microglia, the resident immune cells in the brain, results in release of reactive oxygen metabolites, nitric oxide, and pro-inflammatory cytokines such as tumor necrosis factor- α (TNF- α) and interleukin-1 β (IL-1 β), thereby increasing neuronal loss [19, 20]. It is likely that an increase in reactive oxygen metabolites in the presence of deficient antioxidant mechanisms occurs in the brain of subjects with PD. Thus, increased lipid peroxidation, protein carbonyls, oxidative DNA damage, and evidence of oxidative modification of the respiratory chain complex I have been found in these cases [15, 16, 21–23].

Brilliant blue G dye, also known as Coomassie brilliant blue, is used as a food additive and in biomedicine for staining proteins [24]. Recently, however, studies suggested a potential clinical application for brilliant blue G in the treatment of a number of pathologies involving the brain in experimental models of traumatic brain injury [25], Huntington's disease [26], amyotrophic lateral sclerosis [27, 28], and PD disease [29]. Brilliant blue G is a purinergic P2X7 receptor antagonist. P2X7 receptors are integral plasma membrane proteins, sensitive to activation by ATP. These receptors belong to the family of ionotropic P2X receptors and are expressed in neurons and microglia cells, and modulate synaptic functions and neuronal survival [30]. Stimulation of P2X7 receptors results in Ca^{2+} influx and consequent excitotoxicity, release of cytokines, increased generation of reactive oxygen metabolites, and cell death [31]. The aim of this study was therefore to investigate the ability of brilliant blue G to prevent neuronal damage caused by rotenone in the rat brain. Rotenone is a pesticide of plant origin that is used in rodents to model human idiopathic PD [32, 33].

2. MATERIALS AND METHODS

2.1. Animals

Male Sprague-Dawley rats from the animal house of the National Research Centre (Cairo, Egypt), weighing 180–200 g, were used. Rats were group-housed under temperature- and light-controlled conditions and allowed standard laboratory rodent chow and

water ad libitum. Animal procedures followed the recommendations of the Ethics Committee of the National Research Centre (Cairo, Egypt) and the United States National Institutes of Health Guide for Care and Use of Laboratory Animals (Publication No. 85-23, revised 1985).

2.2. Drugs and Chemicals

Rotenone and brilliant blue G were purchased from Sigma-Aldrich (St Louis, MO, USA). Rotenone was dissolved in dimethyl sulfoxide. Brilliant blue G was dissolved in normal saline.

2.3. Study Design

Rats were randomly divided into five equal groups, with six rats in each group. Group 1 received the vehicle (dimethyl sulfoxide); group 2 received a subcutaneous injection (sc) of rotenone 1.5 mg/kg; groups 3 and 4 received rotenone 1.5 mg/kg subcutaneously along with brilliant blue G at 5 and 10 mg/kg (sc), respectively. The fifth group received only brilliant blue G 10 mg/kg (no rotenone). Drugs were given every other day for 2 weeks. Rats were then euthanized by decapitation for tissue collection; their brains were quickly removed out on an ice-cold plate, washed with ice-cold phosphate-buffered saline (PBS) (pH 7.4), weighed, and stored at -80°C until further biochemical studies. The tissues were homogenized in 0.1 M phosphate-buffered saline (pH 7.4) to give a final concentration of 10% weight/volume (w/v) for the biochemical assays.

2.4. Biochemical Analyses

2.4.1. Determination of Lipid Peroxidation

Lipid peroxidation in the brain homogenates was assayed by measuring the level of malondialdehyde (MDA) using the method of Ruiz-Larrea et al. [34]. In this assay, thiobarbituric acid (TBA) reactive substances (primarily MDA) react with TBA to form TBA-MDA adduct, which can be measured colorimetrically at 532 nm.

2.4.2. Determination of Reduced Glutathione

Reduced glutathione (GSH) was determined in brain homogenates using the method of Ellman et al. [35].

The procedure is based on the reduction of Ellman's reagent 5,5'-dithiobis(2-nitrobenzoic acid) (DTNB) by the free sulfhydryl group on GSH to form yellow colored 5-thio-2-nitrobenzoic acid which can be determined spectrophotometrically at 412 nm.

2.4.3. Determination of Nitric Oxide

Nitric oxide was determined using a colorimetric assay according to the method of Moshage et al. [36]. Nitrate is converted to nitrite via nitrate reductase. Griess reagent then acts to convert nitrite to a deep purple azo compound that can be determined using a spectrophotometer [37].

2.4.4. Determination of Paraoxonase-1 Activity

Paraoxonase-1 (PON-1) arylesterase activity was measured using phenylacetate as a substrate and the formation of phenol was measured spectrophotometrically by monitoring the increase in absorbance at 270 nm at 25°C. One unit of arylesterase activity is defined as 1 μmol of phenol formed per minute. Enzyme activity was calculated based on the extinction coefficient of phenol of $1,310 \text{ M}^{-1} \text{ cm}^{-1}$ at 270 nm, pH 8.0, and 25°C, and expressed as kilo-international unit/liter (kU/l) [37, 38].

2.4.5. Quantification of Nuclear Factor kappaB

Nuclear factor kappaB (NF- κ B) was measured in supernatants using a commercially available human NF- κ B ELISA kit (Glory Science, Del Rio, TX, USA) according to the manufacturer's instructions. The kit uses a double antibody sandwich enzyme linked immunosorbent assay to measure the level of NF- κ B.

2.5. Histopathological Assessment Studies

Brain samples of all animals were dissected immediately after death. The specimens were then fixed in 10% neutral-buffered formalin saline for at least 72 h. All the specimens were washed in tap water for 30 min and then dehydrated in ascending grades of alcohol, cleared in xylene, and embedded in paraffin. Serial sections of 6 μm thickness were cut and stained with hematoxylin and eosin (H&E) for histopathological investigation. Images were examined and photographed under a digital camera (Micro-

scope Digital Camera DP70, Tokyo, Japan), and processed using Adobe Photoshop version 8.0.

2.6. Immunohistochemistry for Caspase-3 and Glial Fibrillary Acidic Protein

Paraffin-embedded brain sections were deparaffinized and hydrated. Immunohistochemistry was performed with mouse monoclonal antibodies against caspase-3 and glial fibrillary acidic protein (GFAP) for detection of the caspase cleavage and GFAP activity. The paraffin sections were heated in a microwave oven (25 min at 720 W) for antigen retrieval and incubated with either anti-caspase or anti-GFAP antibodies (1:50 dilution) overnight at 4°C. After washing with PBS, followed by incubation with biotinylated goat-anti-rabbit immunoglobulin G secondary antibodies (1:200 dilution; Dako Corp, Carpinteria, CA, USA) and streptavidin/alkaline phosphatase complex (1:200 dilution; Dako) for 30 min at room temperature, the binding sites of antibody were visualized with 3,3'-diaminobenzidine DAB (Sigma-Aldrich). After washing with PBS, the samples were counterstained with H&E for 2–3 min, and dehydrated by transferring them through increasing ethanol solutions (30%, 50%, 70%, 80%, 95%, and 100% ethanol). Following dehydration, the slices were soaked twice in xylene at room temperature for 5 min, mounted, examined, and evaluated by a high-power light microscope.

2.7. Immunomorphometric Analysis

The morphometric analysis was performed at the Pathology Department of the National Research Center (Cairo, Egypt), using the Leica Qwin 500 Image Analyzer (LEICA Imaging Systems, Cambridge, UK) which consists of a Leica DM-LB microscope with a JVC color video camera attached to a computer system Leica Q 500IW.

2.8. Detection of Caspase-3 and GFAP Percentage Area

The morphometric analysis is carried out on GFAP and caspase-3 stained slides. The area is determined as an area per field in micrometer square, area fraction, and area percentage by using the interactive software of the system. The area was measured in 10 fields in each slide.

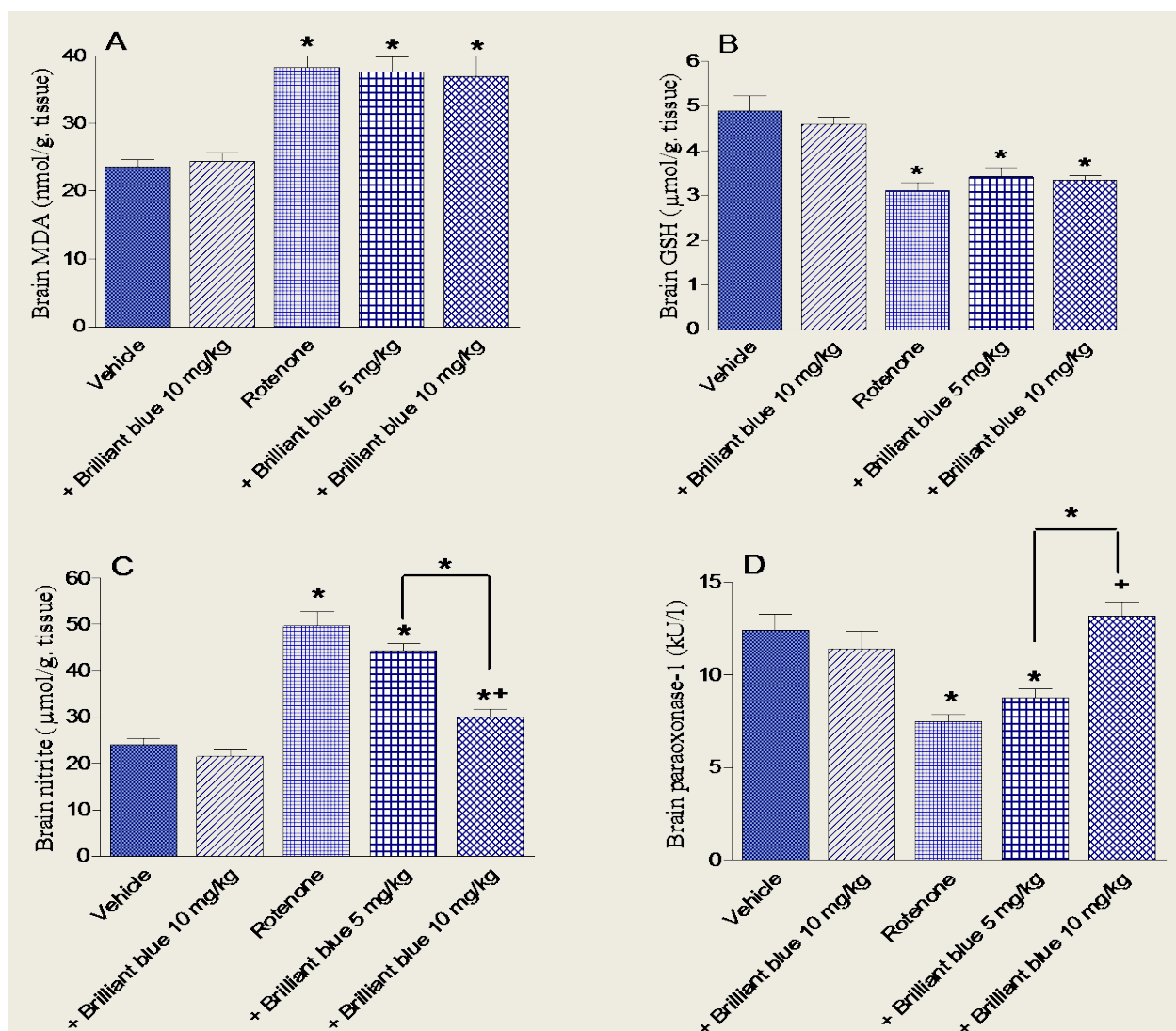


FIGURE 1. Effect of brilliant blue G on malondialdehyde (MDA), reduced glutathione (GSH), nitric oxide, and paraoxonase-1 (PON-1) activity in the brain of vehicle- or rotenone-treated rats. *, $p < 0.05$ versus vehicle-treated group and between other groups as shown in the graph; +, $p < 0.05$ versus rotenone only group.

2.9. Statistical Analysis

Data are presented as mean \pm SEM. Statistical significance was determined using one-way analysis of variance (ANOVA) followed by Duncan's multiple range test using SPSS software (SAS Institute, Cary, NC, USA). A probability value of less than 0.05 was considered statistically significant.

3. RESULTS

3.1. Oxidative Stress

The administration of brilliant blue G alone at 10 mg/kg had no significant effect on brain MDA, GSH, or nitric oxide levels. Rotenone led to marked and significant increase in brain MDA by 62.0% com-

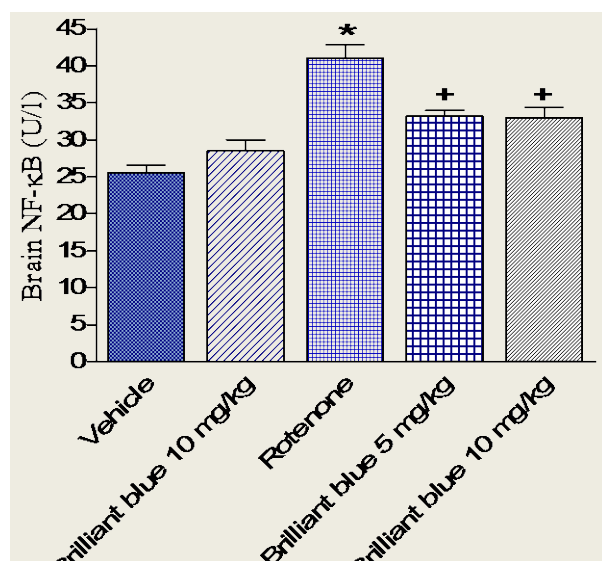


FIGURE 2. Effect of brilliant blue G on nuclear factor kappaB (NF-κB) in vehicle- or rotenone-treated rats. *, $p < 0.05$ versus corresponding vehicle-treated group; +, $p < 0.05$ versus rotenone control group.

pared with the vehicle treated group (38.3 ± 1.6 versus 23.64 ± 1.0 nmol/g tissue) (Figure 1A). Meanwhile, a significant decrease in GSH content by 36.7% was observed in the brain tissue of rotenone-treated rats compared with their vehicle treated counterparts (3.1 ± 0.19 versus 4.9 ± 0.32 μmol/g tissue) (Figure 1B). There was also significant increase in brain nitric oxide by 107.1% compared with the vehicle control group (49.7 ± 3.1 versus 24.0 ± 1.5 μmol/g.tissue) (Figure 1C).

In rats treated with rotenone, brilliant blue G given at 5 or 10 mg/kg showed no significant effect on brain MDA or GSH levels (Figure 1A and 1B). In contrast, brilliant blue G at 10 mg/kg resulted in significant decrease in nitric oxide level by 39.6% compared with the rotenone only group (30.0 ± 1.7 versus 49.7 ± 3.1 μmol/g tissue) (Figure 1C).

3.2. PON-1 Activity

In vehicle-treated rats, brilliant blue G alone at 10 mg/kg had no significant effect on brain PON-1 activity. A significant decrease in PON-1 activity by 39.8% occurred in rats treated with rotenone com-

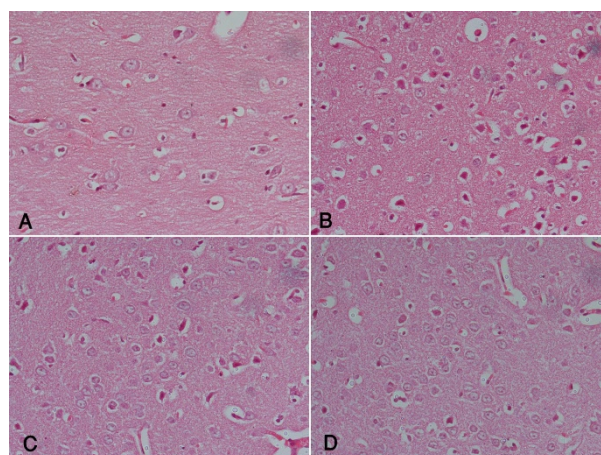


FIGURE 3. Photomicrographs of cerebral cortex sections. (A): Vehicle-treated group, showing the normal structure of the tissue. (B): Rotenone only group. The majority of neurons appeared small and deeply stained in comparison with vehicle-treated group. (C): Rotenone + brilliant blue G 5 mg/kg group. Some affected neurons appeared small in size and deeply stained. (D): Rotenone + brilliant blue G 10 mg/kg group. Remarkable amelioration of rotenone effect was noticed as only a few neurons appeared small. H&E staining with a magnification scale of $\times 400$.

pared with the vehicle group (7.48 ± 0.39 versus 12.43 ± 0.86 kU/l). Brilliant blue G given at 10 mg/kg to rotenone treated rats resulted in restoration of the enzyme activity to normal value (Figure 1D).

3.3. Nuclear Factor kappaB

In vehicle-treated rats, brilliant blue G alone had no significant effect on brain NF-κB. Rotenone resulted in significant increase in NF-κB by 60.8% compared to controls (41.0 ± 1.8 versus 25.5 ± 1.0 U/l). In rotenone-treated rats, brilliant blue G given at 5 or 10 mg/kg resulted in 19.1 and 19.5% decreases in NF-κB, respectively (33.17 ± 0.82 and 33.0 ± 1.4 versus 41.0 ± 1.8 U/l) (Figure 2).

3.4. Histopathological Results

Hematoxylin and eosin staining of cerebral cortex sections from vehicle-treated rats showed normal ap-

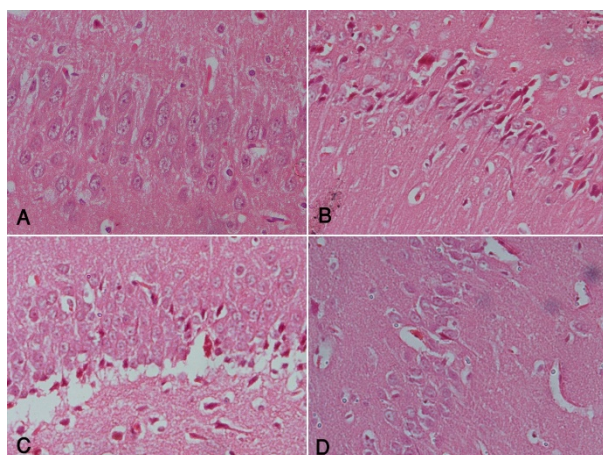


FIGURE 4. Photomicrographs of sections of the hippocampal area. (A): Vehicle-treated group, showing the normal structure of the tissue. (B): Rotenone only group, showing many atrophied deeply stained neurons and disarrangement of the layers of cells. (C): Rotenone + brilliant blue G 5 mg/kg group. There was restoration of the normal architecture of hippocampal area although some affected neurons were still observed. (D): Rotenone + brilliant blue G 10 mg/kg group, showing quite normal structure with only a very few affected cells. H&E staining with a magnification scale of $\times 400$.

pearance (**Figure 3A**). Rotenone caused cerebral cortex neurons to become smaller in size than normal and darkly-stained, denoting a certain level of degeneration (**Figure 3B**). Brilliant blue G given to rotenone-treated rats at 5 mg/kg ameliorated this damaging effect (**Figure 3C**). Better effect was obtained after 10 mg/kg brilliant blue G (**Figure 3D**). Similar results were recorded while examining the hippocampal area (**Figure 4**). Examination of substantia nigra area emphasized the toxic effect of rotenone on this tissue, as the number of pigmented neurons was markedly reduced by the toxicant compared with the normal vehicle-treated tissue (**Figure 5A** and **5B**). The administration of brilliant blue G ameliorated this toxic effect in a dose-dependent manner (**Figure 5C** and **5D**).

3.5. Immunohistochemistry Results

The vehicle treated group showed negligible cleaved caspase-3-positive cells (**Figure 6A**). Rotenone

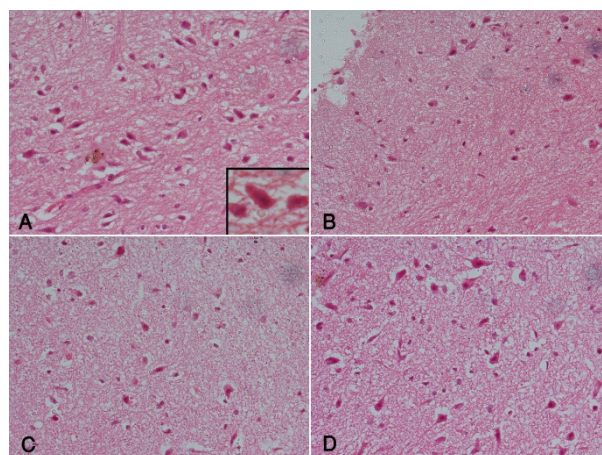


FIGURE 5. Photomicrographs of sections of the substantia nigra. (A): Vehicle-treated group, showing the normal structure of the tissue. (B): Rotenone only group, showing marked decrease in pigmented neurons. (C): Rotenone + brilliant blue G 5 mg/kg group, showing mild restoration of the pigmented neurons. (D) Rotenone + brilliant blue G 10 mg/kg group. There was marked increase in pigmented neurons close to normal. H&E staining with a magnification scale of $\times 400$ except for the inserted box.

caused marked cleaved caspase-3 immunostaining in the cerebral cortex indicating increased apoptosis (**Figure 6B**). Weak caspase-3 immunoreaction was observed after treatment with brilliant blue G as the number of positively stained cells decreased dose-dependently (**Figure 6C** and **6D**). Results for GFAP immunoreactivity confirmed those of caspase-3; the biggest number of astrocytes that appeared with positive reaction was seen in the vehicle-treated group (**Figure 7A**) while the lowest number was observed in the rotenone only-treated group (**Figure 7B**). Brilliant blue G rescued astrocytes: the number of positively stained astrocytes was increased by the dye in a dose-dependent manner (**Figure 7C** and **7D**).

3.6. Immunomorphometric Results

Active caspase-3 labeling was specific in delineating morphologically apoptotic cells, where its expression was localized in the cytoplasm of the apoptotic cells. There was negligible caspase-3 expression in the vehicle treated group with the % area being $2.19 \pm$

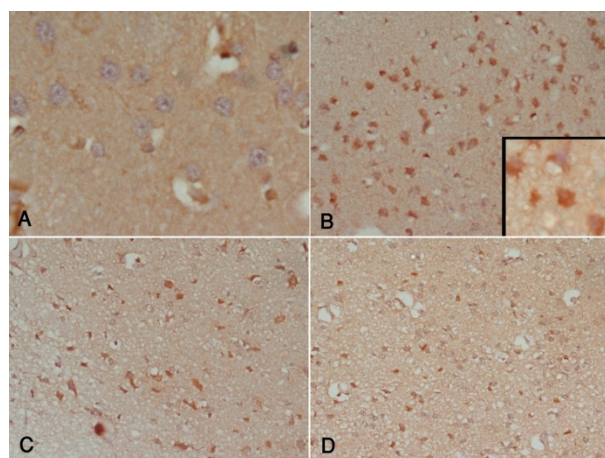


FIGURE 6. Photomicrographs of cerebral cortex sections stained with caspase-3 antibody. (A) Vehicle-treated group, showing negative reaction to the stain in almost all of the cells. (B): Rotenone only group, showing many neurons with positive reaction that also appeared smaller in size compared with the vehicle-treated group. (C): Rotenone + brilliant blue G 5 mg/kg group, showing slight reduction in positively stained neurons. (D): Rotenone + brilliant blue G 10 mg/kg group, showing marked reduction of positively stained neurons. Magnification scale: $\times 400$ except for the inserted box.

0.41. In contrast, the maximum caspase-3 expression was seen in the rotenone only group (% area: 44.5 ± 3.7). Caspase-3 immunoreactivity decreased by brilliant blue G in a dose dependent manner. There were 60.4% and 83.6% decrease in % area by 5 and 10 mg/kg brilliant blue G, respectively (17.6 ± 1.13 and 7.29 ± 0.44 versus 44.5 ± 3.7) (**Figures 8 and 9**).

Further histopathological evaluation was done via quantitative morphometric analysis of the pathological changes using GFAP, which was detected in the cytoplasm of viable astrocytes. The maximum expression of GFAP was seen in the vehicle treated group while the lowest GFAP expression occurred in the rotenone only group, thereby, indicating its destructive effect on neuronal tissue (40.5 ± 3.2 versus 4.45 ± 0.51). The % area of GFAP showed marked increments in the groups treated with rotenone combined with brilliant blue G, with the effect being dose-dependent (11.65 ± 0.9 and 35.44 ± 1.2 versus 4.45 ± 0.51) (**Figures 10 and 11**).

4. DISCUSSION

In this study, the administration of rotenone induced brain oxidative stress as evidenced by the increment in the level of the lipid peroxidation product malondialdehyde indicating free radical attack on membrane lipids [11]. Reduced glutathione, an important intracellular antioxidant and a free radical scavenger [39] showed marked decrease in the brain of rotenone treated rats, possibly reflecting consumption of the thiol by the increased generation of reactive oxygen metabolites. These findings agree with other studies suggesting increased intracellular reactive oxygen metabolites by rotenone [40, 41]. We also observed markedly increased nitric acid content in the brain of rats treated with rotenone, a finding that is in agreement with previously published data [42]. Rotenone also led to significant decrease in the activity of PON-1 enzyme which is consistent with our previous observations following systemic or intrastriatal injection of this toxin into rodents. PON-1 functions in the detoxification of organophosphorus compounds, by hydrolyzing their active metabolites (oxons) [43]. The activity of this enzyme has been shown to be decreased in the serum of patients with a number of neurological disorders such as dementia [44], multiple sclerosis [45], and autism [46]. The enzyme is endowed with antioxidative and anti-inflammatory properties, and the observed decrease in its activity in the current study is likely to reflect inactivation by the increased level of oxidative stress [47, 48]. On the other hand, the recovery of PON-1 activity after treatment with brilliant blue G might reflect neuroprotection. Studies in animal models of neurodegeneration showed that restoration of PON-1 activity is associated with the improvement in oxidative burden and the extent of neuronal damage [49, 50], thereby, suggesting that the enzyme might be a sensitive indicator of the redox state of the cell.

Being highly lipophilic, rotenone readily crosses the blood brain barrier and inhibits complex I (NADH-ubiquinone reductase) activity in rat brain mitochondria [51]. By inhibiting the mitochondrial complex I activity, rotenone decreases ATP production and increases the formation of superoxide giving rise to oxidative stress and mitochondrial damage, and initiates cell apoptosis [52, 53]. Rotenone treatment did not cause oxidative damage and dopaminergic cell death in cells transduced with nicotinamide-adenine dinucleotide-ubiquinone oxi-

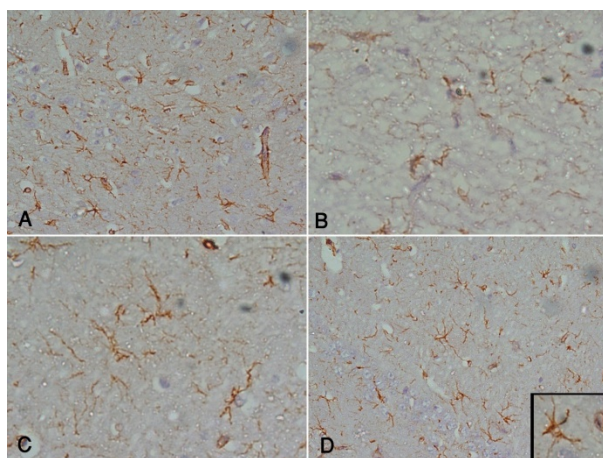


FIGURE 7. Photomicrographs of cerebral cortex sections stained with GFAP antibody. (A): Vehicle-treated group, showing positively stained glial (astrocytes) cells. (B): Rotenone only group, showing marked reduction of glial cells with positive reaction and atrophy of their body. (C): Rotenone + brilliant blue G 5 mg/kg group, showing slight increase in positively stained glial cells, although bodies of most of these cells were still atrophied. (D): Rotenone + brilliant blue G 10 mg/kg group, showing marked increase of positively stained glial cells; most of them regained the normal size of their bodies. $\times 400$ except for the inserted box.

doreductase (Ndi1) of *Saccharomyces cerevisiae* which acts to replace complex I [54, 55]. Rotenone thus evokes neuronal damage by virtue of its ability to increase cellular reactive oxygen metabolites and reactive nitrogen species. In vitro, rotenone causes apoptotic dopaminergic cell death which could be decreased by antioxidants, such as α -tocopherol [56], glutathione, and ascorbate [52] or by the catalase enzyme [57]. We also demonstrated increased levels of NF- κ B in the brain of rotenone intoxicated rats. NF- κ B is a protein transcription factor required for the expression of several proinflammatory mediators, such as inducible nitric oxide synthase (iNOS), cyclooxygenase-2, IL-1 β , IL-6, TNF- α and intracellular adhesion molecules [57]. NF- κ B is kept inactivated in the cytosol by binding to an inhibitory subunit I κ B- α in the non-stimulated condition. It is released from its inhibitory subunit whenever the cell is stimulated by inflammatory and toxic signals, and trans-

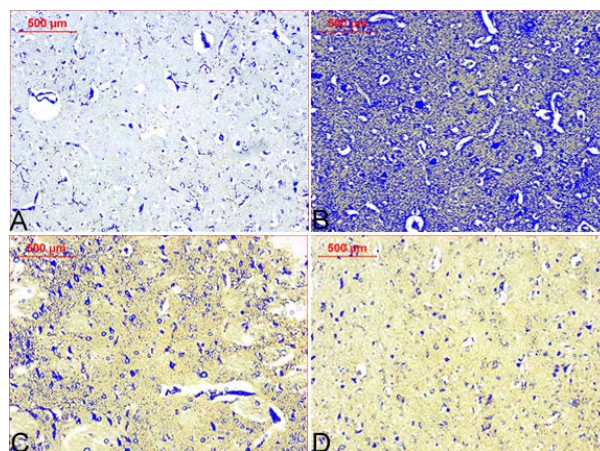


FIGURE 8. Captured photos from the image analyzer system marking the immunoreactivity of brain tissues to cleaved caspase-3 by blue color. (A): vehicle-treated group. (B): Rotenone only group. (C): Rotenone + brilliant blue G 5 mg/kg group. (D): Rotenone + brilliant blue G 10 mg/kg group.

locates to the nucleus and activates the transcription of genes encoding proinflammatory mediators and proinflammatory cytokines [58, 59]. Rotenone has also been shown to result in the increased expression of the proinflammatory cytokine TNF- α in the rat brain [50], thereby, implicating neuroinflammation in the process of cell death caused by the pesticide.

In the present study, we investigated the effect of brilliant blue G, a purinergic P2X7 receptor antagonist on the rat brain oxidative stress and neuronal damage caused by rotenone. Our findings indicate that brilliant blue G by itself at the dose of 10 mg/kg has no significant effect on biochemical indicators of oxidative stress, nitric oxide concentrations, NF- κ B, or PON-1 activity. In rats treated with rotenone, the dye, however, caused dose-dependent decrease in the brain concentration of nitric oxide, increased PON-1 activity, and decreased NF- κ B level. It is unlikely that the neuroprotective effect of brilliant blue G observed in this study is the result of a decrease in oxidative burden. Our results rather suggest that inhibition of nitric oxide and NF- κ B mediate, at least in part, the brilliant blue G-induced neuroprotection. Rotenone has been shown to induce the expression of iNOS in the rodent substantia nigra and striatum

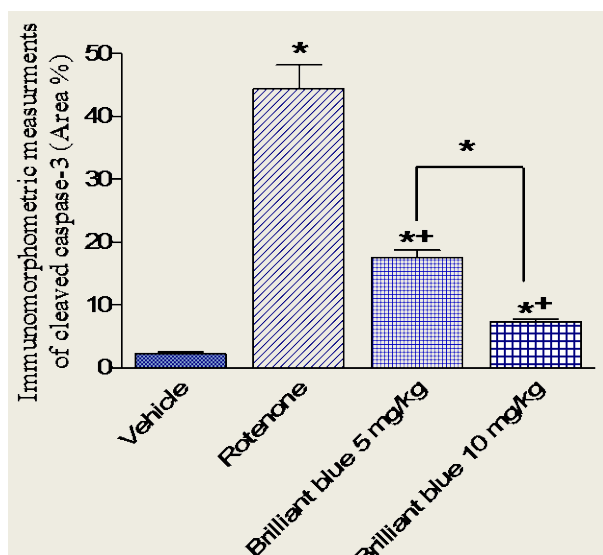


FIGURE 9. Quantitative morphometric analysis of caspase-3 immunoreactivity showing the % area of apoptotic cells (mean \pm SEM). *, $p < 0.05$ versus vehicle-treated group and between other groups as shown in the graph; +, $p < 0.05$ versus rotenone only group.

[49, 60–62], which will result in an increase in intracellular nitric oxide level and oxidative/nitrosative stress with consequent cellular macromolecular damage [63, 64]. Nitric oxide has been suggested to have an important role in neurodegenerative changes caused by rotenone as well as other toxins implicated in the development of Parkinson's disease [60, 61]. In this context, inhibition of neuronal NOS (nNOS) activity with 7-nitroindazole resulted in decreased 3-nitrotyrosine level and afforded protection against nigrostriatal damage induced by rotenone in the rat brain [60]. It has also been shown that nNOS inhibition or lack of iNOS due to gene deletion conferred resistance to the neurotoxic action of the nigrostriatal toxin 1-methyl-4-phenyl-1,2,3,6-tetrahydropyridine (MPTP) in mice [65, 66]. Nitric oxide acting via the formation of other reactive oxides of nitrogen such as nitrogen dioxide (NO_2), dinitrogen trioxide (N_2O_3), or the highly reactive peroxynitrite, leads to oxidation, nitration of tyrosine residues in proteins, and nitrosylation of thiols in proteins or reduced glutathione [67, 68].

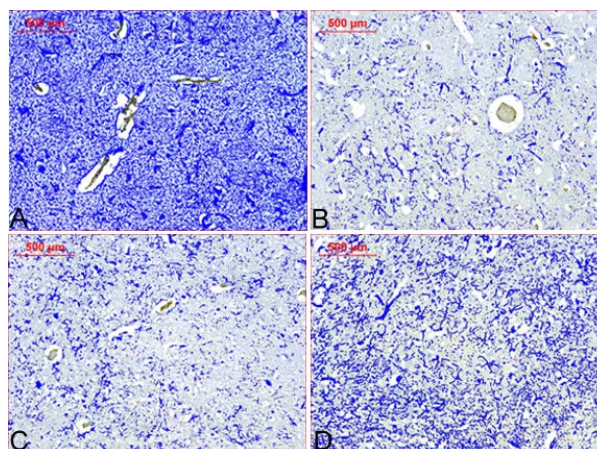


Figure 10. Captured photos from the image analyzer system marking the immunoreactivity of brain tissues to GFAP by blue color. (A): vehicle-treated group. (B): Rotenone only group. (C): Rotenone + brilliant blue G 5 mg/kg group. (D): Rotenone + brilliant blue G 10 mg/kg group.

In this study, histopathological assessment of brain tissue indicated that brilliant blue G given to rotenone intoxicated rats was able to prevent neuronal atrophy in the cerebral cortex and hippocampus. In the substantia nigra, brilliant blue G treatment resulted in the preservation of the pigmented neuromelanin containing neurons. Glia cells (microglia and astrocytes) have been implicated in the process of neuronal loss in Parkinson's disease [19, 20, 69]. Astrocytes are the most abundant type of glial cells in the brain. These cells do not only provide structural and metabolic support to neurons, but are involved in regulating synaptic transmission and plasticity, and in maintaining local cerebral blood flow [70]. Astrocytes express GFAP, a structural protein in glial filaments that maintains their cytoskeleton [71] and a marker for their activation during central nervous system injury from ischemia, trauma, or toxins [72]. In the present work, GFAP expression was measured in the cerebral cortex by immunohistochemical labeling. Our results indicated that rotenone caused marked decrease in the number of GFAP-positive astrocytes, suggesting induction of astrocyte cell death by the toxicant. This reduction in GFAP-positive cells was prevented by brilliant blue G, which reflects a neuroprotective effect.

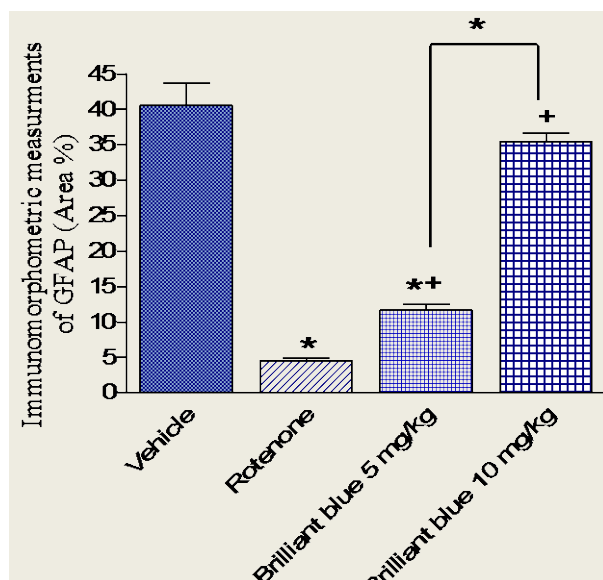


Figure 11. Quantitative morphometric analysis of glial fibrillary acidic protein (GFAP) expression in the cytoplasm of viable astrocytes measured as % area of viable astrocytic cells (mean \pm SEM). *, $p < 0.05$ versus vehicle-treated group and between other groups as shown in the graph; +, $p < 0.05$ versus rotenone only group.

Caspases are aspartate-specific cysteine proteases involved in the initiation and execution of apoptosis, a morphologically distinct form of cell death [73, 74]. Rotenone caused marked active caspase-3 immunoreactivity in the cerebral cortex which is consistent with other studies showing similar effect for the pesticide in the substantia nigra, striatum, and cerebral cortex, and suggesting increased neuronal apoptosis as a mechanism of cell death by the toxicant [50, 62, 75, 76]. Caspase-3 immunoreactivity and the area of apoptotic cells showed a dose-dependent decrease after treatment with brilliant blue G, suggesting inhibition of caspase-3 activation as a likely mechanism by which the dye affords neuroprotection.

Studies suggested that brilliant blue G might hold promise in the treatment of neurodegenerative disorders. It showed neuroprotective effects in transgenic mouse models of Huntington's disease [26] and amyotrophic lateral sclerosis [27, 28]), and in 6-

hydroxydopamine (6-OHDA)-induced PD in rats [29], and following rat traumatic brain injury [25]. In these studies, brilliant blue G was given at the dose range of 45–50 mg/kg. Several mechanisms have been postulated to account for brilliant blue G-induced neuroprotection, including a decrease in calcium influx, a decrease in microgliosis, NF- κ B, IL-1 β , IL-10, protein kinase C γ and an increase in brain-derived neurotrophic factor [25, 27]. The findings in the present study thus confirm and extend other studies indicating a neuroprotective action of brilliant blue G and suggest that the purinergic P2X7 receptor antagonist acts by reducing apoptosis and neuroinflammation.

ACKNOWLEDGMENTS

The authors declare that there are no conflicts of interest with regard to the studies reported in this manuscript.

REFERENCES

1. Beitz JM. Parkinson's disease: a review. *Front Biosci* (Schol Ed) 2014; 6:65–74.
2. Abdel-Salam OME. Drug therapy for Parkinson's disease: an update. *World J Pharmacol* 2015; 4(1):117–43.
3. Kumar KR, Djarmati-Westenberger A, Grunewald A. Genetics of Parkinson's disease. *Semin Neurol* 2011; 31(5):433–40. doi: 10.1055/s-0031-1299782.
4. Abdel-Salam OM. The paths to neurodegeneration in genetic Parkinson's disease. *CNS Neurol Disord Drug Targets* 2014; 13(9):1485–512.
5. Wirdefeldt K, Adami HO, Cole P, Trichopoulos D, Mandel J. Epidemiology and etiology of Parkinson's disease: a review of the evidence. *Eur J Epidemiol* 2011; 26 Suppl 1:S1–58. doi: 10.1007/s10654-011-9581-6.
6. Hughes AJ, Daniel SE, Kilford L, Lees AJ. Accuracy of clinical diagnosis of idiopathic Parkinson's disease: a clinico-pathological study of 100 cases. *J Neurol Neurosurg Psychiatry* 1992; 55(3):181–4.
7. Fahn S. Description of Parkinson's disease as a clinical syndrome. *Ann N Y Acad Sci* 2003;

- 991:1–14.
8. Drechsel DA, Patel M. Role of reactive oxygen species in the neurotoxicity of environmental agents implicated in Parkinson's disease. *Free Radic Biol Med* 2008; 44(11):1873–86. doi: 10.1016/j.freeradbiomed.2008.02.008.
9. Miller RL, James-Kracke M, Sun GY, Sun AY. Oxidative and inflammatory pathways in Parkinson's disease. *Neurochem Res* 2009; 34(1):55–65. doi: 10.1007/s11064-008-9656-2.
10. Halliwell B. Role of free radicals in the neurodegenerative diseases: therapeutic implications for antioxidant treatment. *Drugs Aging* 2001; 18(9):685–716.
11. Halliwell B, Gutteridge JM. *Free Radicals in Biology and Medicine*. 2nd edition. Clarendon Press, Oxford, UK. 1989.
12. Floyd RA. Antioxidants, oxidative stress, and degenerative neurological disorders. *Proc Soc Exp Biol Med* 1999; 222(3):236–45.
13. Sulzer D, Zecca L. Intraneuronal dopamine-quinone synthesis: a review. *Neurotox Res* 2000; 1(3):181–95.
14. Bolton JL, Dunlap T. Formation and Biological Targets of Quinones: Cytotoxic versus Cytoprotective Effects. *Chem Res Toxicol* 2017; 30(1):13–37. doi: 10.1021/acs.chemrestox.6b00256.
15. Parker WD, Jr., Boyson SJ, Parks JK. Abnormalities of the electron transport chain in idiopathic Parkinson's disease. *Ann Neurol* 1989; 26(6):719–23. doi: 10.1002/ana.410260606.
16. Keeney PM, Xie J, Capaldi RA, Bennett JP, Jr. Parkinson's disease brain mitochondrial complex I has oxidatively damaged subunits and is functionally impaired and misassembled. *J Neurosci* 2006; 26(19):5256–64. doi: 10.1523/JNEUROSCI.0984-06.2006.
17. Ramsay RR, Kowal AT, Johnson MK, Salach JJ, Singer TP. The inhibition site of MPP+, the neurotoxic bioactivation product of 1-methyl-4-phenyl-1,2,3,6-tetrahydropyridine is near the Q-binding site of NADH dehydrogenase. *Arch Biochem Biophys* 1987; 259(2):645–9.
18. Perier C, Tieu K, Guegan C, Caspersen C, Jackson-Lewis V, Carelli V, et al. Complex I deficiency primes Bax-dependent neuronal apoptosis through mitochondrial oxidative damage. *Proc Natl Acad Sci USA* 2005; 102(52):19126–31. doi: 10.1073/pnas.0508215102.
19. Block ML, Hong JS. Chronic microglial activation and progressive dopaminergic neurotoxicity. *Biochem Soc Trans* 2007; 35(Pt 5):1127–32. doi: 10.1042/BST0351127.
20. Lull ME, Block ML. Microglial activation and chronic neurodegeneration. *Neurotherapeutics* 2010; 7(4):354–65. doi: 10.1016/j.nurt.2010.05.014.
21. Dexter DT, Holley AE, Flitter WD, Slater TF, Wells FR, Daniel SE, et al. Increased levels of lipid hydroperoxides in the parkinsonian substantia nigra: an HPLC and ESR study. *Mov Disord* 1994; 9(1):92–7. doi: 10.1002/mds.870090115.
22. Zhang J, Perry G, Smith MA, Robertson D, Olson SJ, Graham DG, et al. Parkinson's disease is associated with oxidative damage to cytoplasmic DNA and RNA in substantia nigra neurons. *Am J Pathol* 1999; 154(5):1423–9. doi: 10.1016/S0002-9440(10)65396-5.
23. Alam ZI, Daniel SE, Lees AJ, Marsden DC, Jenner P, Halliwell B. A generalised increase in protein carbonyls in the brain in Parkinson's but not incidental Lewy body disease. *J Neurochem* 1997; 69(3):1326–9.
24. Ferreira LG, Faria RX, Ferreira NC, Soares-Bezerra RJ. Brilliant blue dyes in daily food: how could purinergic system be affected? *Int J Food Sci* 2016; 2016:7548498. doi: 10.1155/2016/7548498.
25. Wang YC, Cui Y, Cui JZ, Sun LQ, Cui CM, Zhang HA, et al. Neuroprotective effects of brilliant blue G on the brain following traumatic brain injury in rats. *Mol Med Rep* 2015; 12(2):2149–54. doi: 10.3892/mmr.2015.3607.
26. Diaz-Hernandez M, Diez-Zaera M, Sanchez-Nogueiro J, Gomez-Villafuertes R, Canals JM, Alberch J, et al. Altered P2X7-receptor level and function in mouse models of Huntington's disease and therapeutic efficacy of antagonist administration. *FASEB J* 2009; 23(6):1893–906. doi: 10.1096/fj.08-122275.
27. Apolloni S, Amadio S, Parisi C, Matteucci A, Potenza RL, Armida M, et al. Spinal cord pathology is ameliorated by P2X7 antagonism in a SOD1-mutant mouse model of amyotrophic lateral sclerosis. *Dis Model Mech* 2014; 7(9):1101–9. doi: 10.1242/dmm.017038.

28. Cervetto C, Frattaroli D, Maura G, Marcoli M. Motor neuron dysfunction in a mouse model of ALS: gender-dependent effect of P2X7 antagonism. *Toxicology* 2013; 311(1–2):69–77. doi: 10.1016/j.tox.2013.04.004.
29. Carmo MR, Menezes AP, Nunes AC, Pliassova A, Rolo AP, Palmeira CM, et al. The P2X7 receptor antagonist Brilliant Blue G attenuates contralateral rotations in a rat model of Parkinsonism through a combined control of synaptotoxicity, neurotoxicity and gliosis. *Neuropharmacology* 2014; 81:142–52. doi: 10.1016/j.neuropharm.2014.01.045.
30. Anderson CM, Nedergaard M. Emerging challenges of assigning P2X7 receptor function and immunoreactivity in neurons. *Trends Neurosci* 2006; 29(5):257–62. doi: 10.1016/j.tins.2006.03.003.
31. Sperlagh B, Illes P. P2X7 receptor: an emerging target in central nervous system diseases. *Trends Pharmacol Sci* 2014; 35(10):537–47. doi: 10.1016/j.tips.2014.08.002.
32. Betarbet R, Sherer TB, MacKenzie G, Garcia-Osuna M, Panov AV, Greenamyre JT. Chronic systemic pesticide exposure reproduces features of Parkinson's disease. *Nat Neurosci* 2000; 3(12):1301–6. doi: 10.1038/81834.
33. Sherer TB, Kim JH, Betarbet R, Greenamyre JT. Subcutaneous rotenone exposure causes highly selective dopaminergic degeneration and alpha-synuclein aggregation. *Exp Neurol* 2003; 179(1):9–16.
34. Ruiz-Larrea MB, Leal AM, Liza M, Lacort M, de Groot H. Antioxidant effects of estradiol and 2-hydroxyestradiol on iron-induced lipid peroxidation of rat liver microsomes. *Steroids* 1994; 59(6):383–8.
35. Ellman GL. Tissue sulfhydryl groups. *Arch Biochem Biophys* 1959; 82(1):70–7.
36. Moshage H, Kok B, Huizenga JR, Jansen PL. Nitrite and nitrate determinations in plasma: a critical evaluation. *Clin Chem* 1995; 41(6 Pt 1):892–6.
37. Watson AD, Berliner JA, Hama SY, La Du BN, Faull KF, Fogelman AM, et al. Protective effect of high density lipoprotein associated paraoxonase: inhibition of the biological activity of minimally oxidized low density lipoprotein. *J Clin Invest* 1995; 96(6):2882–91. doi: 10.1172/JCI118359.
38. Higashino K, Takahashi Y, Yamamura Y. Release of phenyl acetate esterase from liver microsomes by carbon tetrachloride. *Clin Chim Acta* 1972; 41:313–20.
39. Bains JS, Shaw CA. Neurodegenerative disorders in humans: the role of glutathione in oxidative stress-mediated neuronal death. *Brain Res Brain Res Rev* 1997; 25(3):335–58.
40. Liu HQ, Zhu XZ, Weng EQ. Intracellular dopamine oxidation mediates rotenone-induced apoptosis in PC12 cells. *Acta Pharmacol Sin* 2005; 26(1):17–26. doi: 10.1111/j.1745-7254.2005.00003.x.
41. Choi WS, Palmiter RD, Xia Z. Loss of mitochondrial complex I activity potentiates dopamine neuron death induced by microtubule dysfunction in a Parkinson's disease model. *J Cell Biol* 2011; 192(5):873–82. doi: 10.1083/jcb.201009132.
42. Xiong ZK, Lang J, Xu G, Li HY, Zhang Y, Wang L, et al. Excessive levels of nitric oxide in rat model of Parkinson's disease induced by rotenone. *Exp Ther Med* 2015; 9(2):553–8. doi: 10.3892/etm.2014.2099.
43. La Du BN. Human serum paraoxonase/arylesterase. In: *Pharmacogenetics of Drug Metabolism* (W Kalow). Pergamon Press, Elmford, NY, USA. 1992. pp. 51–91.
44. Wehr H, Bednarska-Makaruk M, Graban A, Lipczynska-Lojkowska W, Rodo M, Bochynska A, et al. Paraoxonase activity and dementia. *J Neurol Sci* 2009; 283(1–2):107–8. doi: 10.1016/j.jns.2009.02.317.
45. Jamroz-Wisniewska A, Beltowski J, Stelmasiak Z, Bartosik-Psujek H. Paraoxonase 1 activity in different types of multiple sclerosis. *Mult Scler* 2009; 15(3):399–402. doi: 10.1177/1352458508098371.
46. Abdel-Salam OME, Youness ER, Mohammed NA, Abu Elhamed WA. Nuclear factor-kappa B and other oxidative stress biomarkers in serum of autistic children. *Open J Mol Integ Physiol* 2015; 5:18–27.
47. Aviram M, Rosenblat M, Billecke S, Eroglu J, Sorenson R, Bisgaier CL, et al. Human serum paraoxonase (PON 1) is inactivated by oxidized low density lipoprotein and preserved by antioxidants. *Free Radic Biol Med* 1999; 26(7–8):892–904.
48. Nguyen SD, Sok DE. Preferential inhibition of

- paraoxonase activity of human paraoxonase 1 by negatively charged lipids. *J Lipid Res* 2004; 45(12):2211–20. doi: 10.1194/jlr.M400144-JLR200.
49. Abdel-Salam OME, Mohammed NA, Youness ER, Khadrawy YA, Omara EA, Sleem AA. Cerebrolysin protects against rotenone-induced oxidative stress and neurodegeneration. *J Neurorestoratol* 2014; 2:47–63.
 50. Abdel-Salam OME, Mohammed NA, Youness ER, Khadrawy YA, Omara EA, Sleem AA. Rotenone-induced nigrostriatal toxicity is reduced by methylene blue. *J Neurorestoratol* 2014; 2:65–80.
 51. Richardson JR, Quan Y, Sherer TB, Greenamyre JT, Miller GW. Paraquat neurotoxicity is distinct from that of MPTP and rotenone. *Toxicol Sci* 2005; 88(1):193–201. doi: 10.1093/toxsci/kfi304.
 52. Li N, Ragheb K, Lawler G, Sturgis J, Rajwa B, Melendez JA, et al. Mitochondrial complex I inhibitor rotenone induces apoptosis through enhancing mitochondrial reactive oxygen species production. *J Biol Chem* 2003; 278(10):8516–25. doi: 10.1074/jbc.M210432200.
 53. Grivennikova VG, Vinogradov AD. Generation of superoxide by the mitochondrial complex I. *Biochim Biophys Acta* 2006; 1757(5–6):553–61. doi: 10.1016/j.bbabi.2006.03.013.
 54. Seo BB, Marella M, Yagi T, Matsuno-Yagi A. The single subunit NADH dehydrogenase reduces generation of reactive oxygen species from complex I. *FEBS Lett* 2006; 580(26):6105–8. doi: 10.1016/j.febslet.2006.10.008.
 55. Marella M, Seo BB, Nakamaru-Ogiso E, Greenamyre JT, Matsuno-Yagi A, Yagi T. Protection by the NDI1 gene against neurodegeneration in a rotenone rat model of Parkinson's disease. *PLoS One* 2008; 3(1):e1433. doi: 10.1371/journal.pone.0001433.
 56. Testa CM, Sherer TB, Greenamyre JT. Rotenone induces oxidative stress and dopaminergic neuron damage in organotypic substantia nigra cultures. *Brain Res Mol Brain Res* 2005; 134(1):109–18. doi: 10.1016/j.molbrainres.2004.11.007.
 57. Zhou Q, Liu C, Liu W, Zhang H, Zhang R, Liu J, et al. Rotenone induction of hydrogen peroxide inhibits mTOR-mediated S6K1 and 4E-BP1/eIF4E pathways, leading to neuronal apoptosis. *Toxicol Sci* 2015; 143(1):81–96. doi: 10.1093/toxsci/kfu211.
 58. Blackwell TS, Christman JW. The role of nuclear factor-kappa B in cytokine gene regulation. *Am J Respir Cell Mol Biol* 1997; 17(1):3–9. doi: 10.1165/ajrcmb.17.1.f132.
 59. Memet S. NF-kappaB functions in the nervous system: from development to disease. *Biochem Pharmacol* 2006; 72(9):1180–95. doi: 10.1016/j.bcp.2006.09.003.
 60. He Y, Imam SZ, Dong Z, Jankovic J, Ali SF, Appel SH, et al. Role of nitric oxide in rotenone-induced nigro-striatal injury. *J Neurochem* 2003; 86(6):1338–45.
 61. Bashkatova V, Alam M, Vanin A, Schmidt WJ. Chronic administration of rotenone increases levels of nitric oxide and lipid peroxidation products in rat brain. *Exp Neurol* 2004; 186(2):235–41. doi: 10.1016/j.expneurol.2003.12.005.
 62. Abdel-Salam OME, Omara EA, El-Shamarka ME-S, Hussein JS. Nigrostriatal damage after systemic rotenone and/or lipopolysaccharide and the effect of cannabis. *Comp Clin Pathol* 2014; 23:1343–58.
 63. Moncada S, Palmer RM, Higgs EA. Nitric oxide: physiology, pathophysiology, and pharmacology. *Pharmacol Rev* 1991; 43(2):109–42.
 64. Wink DA, Mitchell JB. Chemical biology of nitric oxide: Insights into regulatory, cytotoxic, and cytoprotective mechanisms of nitric oxide. *Free Radic Biol Med* 1998; 25(4–5):434–56.
 65. Liberatore GT, Jackson-Lewis V, Vukosavic S, Mandir AS, Vila M, McAuliffe WG, et al. Inducible nitric oxide synthase stimulates dopaminergic neurodegeneration in the MPTP model of Parkinson disease. *Nat Med* 1999; 5(12):1403–9. doi: 10.1038/70978.
 66. Watanabe H, Muramatsu Y, Kurosaki R, Michimata M, Matsubara M, Imai Y, et al. Protective effects of neuronal nitric oxide synthase inhibitor in mouse brain against MPTP neurotoxicity: an immunohistological study. *Eur Neuropsychopharmacol* 2004; 14(2):93–104. doi: 10.1016/S0924-977X(03)00065-8.
 67. Brown GC, Borutaite V. Nitric oxide, mitochondria, and cell death. *IUBMB Life* 2001; 52(3–5):189–95. doi:

- 10.1080/15216540152845993.
68. Brown GC. Nitric oxide and neuronal death. *Nitric Oxide* 2010; 23(3):153–65. doi: 10.1016/j.niox.2010.06.001.
69. Beach TG, Sue LI, Walker DG, Lue LF, Connor DJ, Caviness JN, et al. Marked microglial reaction in normal aging human substantia nigra: correlation with extraneuronal neuromelanin pigment deposits. *Acta Neuropathol* 2007; 114(4):419–24. doi: 10.1007/s00401-007-0250-5.
70. Araque A, Navarrete M. Glial cells in neuronal network function. *Philos Trans R Soc Lond B Biol Sci* 2010; 365(1551):2375–81. doi: 10.1098/rstb.2009.0313.
71. Dahl D, Bignami A. Immunogenic properties of the glial fibrillary acidic protein. *Brain Res* 1976; 116(1):150–7.
72. O'Callaghan JP, Sriram K. Glial fibrillary acidic protein and related glial proteins as biomarkers of neurotoxicity. *Expert Opin Drug Saf* 2005; 4(3):433–42. doi: 10.1517/14740338.4.3.433.
73. Thornberry NA, Lazebnik Y. Caspases: enemies within. *Science* 1998; 281(5381):1312–6.
74. Yuan J, Yankner BA. Apoptosis in the nervous system. *Nature* 2000; 407(6805):802–9. doi: 10.1038/35037739.
75. Ahmadi FA, Linseman DA, Grammatopoulos TN, Jones SM, Bouchard RJ, Freed CR, et al. The pesticide rotenone induces caspase-3-mediated apoptosis in ventral mesencephalic dopaminergic neurons. *J Neurochem* 2003; 87(4):914–21.
76. Abdel-Salam OME, Youness ER, Mohammed NA, Shaffie N, Abouelfadl DM, Sleem AA. The effect of 2,4-dinitrophenol on oxidative stress and neuronal damage in rat brain induced by systemic rotenone injection. *Reactive Oxygen Species* 2017; 3(8):135–47. doi: 10.20455/ros.2017.813.